Available online at www.sciencedirect.com
ScienceDirect
ELSEVIER
Journal of Nuclear Materials 362 (2007) 26–35
journal of nuclear materials
www.elsevier.com/locate/jnucmat

X-ray and thermal studies of the Na–U–Mo–O system

N.D. Dahale *, Meera Keskar, R. Agarwal, K.D. Singh Mudher

Fuel Chemistry Division, B.A.R.C., Trombay, Mumbai 400 085, India

Received 30 June 2006; accepted 17 October 2006

Abstract

In the Na–U–Mo–O system, five compounds with composition $Na_2UMo_2O_{10}$, $Na_2U_2Mo_2O_{13}$, $Na_2U_2Mo_3O_{16}$, $Na_2UMo_4O_{16}$ and $Na_2U_2Mo_4O_{19}$ were prepared by solid state reaction of Na_2MoO_4, UO_3 and MoO_3 in the required stoic-hiometric ratio. The compounds were characterized by X-ray powder diffraction, infrared and thermal analysis techniques. The XRD data of all the above-mentioned compounds were indexed on the orthorhombic system. All the compounds showed thermal stability up to 600 °C in air and decomposed at 950 °C to form $Na_2U_2O_7$. Infrared spectra of all the compounds show strong spectral bands in the range 700–950 cm^{-1} due to MoO_4^{-2} tetrahedra and the UO_2^{2+} group. A pseudo-ternary phase diagram of Na_2O–UO_3–MoO_3 was drawn using the quaternary compounds and information available on Na–U–O, Mo–U–O and Na–Mo–O ternary systems. The various phase fields prepared during this work were established by XRD analysis.

1. Introduction

The liquid metal fast breeder reactor (LMFBR) uses mixed oxide $(U,Pu)O_2$ as fuel, liquid sodium as coolant and stainless steel 316 as cladding material. Molybdenum is an important alloying element in structural steel in the sodium circuits of LMFBRs. It is also an important fission product, formed in large quantity (fission yield around 20%) in a nuclear reactor and is present in the irradiated fuel. When the dissolved oxygen level in liquid sodium exceeds a threshold value, the clad gets corroded due to the reaction of sodium with the cladding components chromium, iron, molybdenum, etc., and various ternary oxides are formed, imparting high temperature creep strength to the clad. The formation of these compounds may be one of the important factors responsible for the change in behaviour of the nuclear fuel which limit the life of fuel pin. Thus structural and thermal studies on the sodium–uranium–molybdenum–oxygen (Na–U–Mo–O) system are important for understanding the fuel–clad–coolant chemical interaction in LMFBR [1].

The quaternary systems, alkali metal–U–Mo–O, have been studied by various workers. In the study of the K–U–Mo–O system, Dion and Noel [2,3] prepared and identified new phases, namely,

---

* Corresponding author. Fax: +91 22 25505345.
E-mail address: nddahale@apsara.barc.ernet.in (N.D. Dahale).

0022-3115/$ - see front matter © 2006 Elsevier B.V. All rights reserved.
doi:10.1016/j.jnucmat.2006.10.020

$K_2UO_2(MoO_4)_2$, $K_2(UO_2)_2(MoO_4)_3$, $K_6(UO_2)(MoO_4)_4$, $K_2(UO_2)_3(MoO_4)_4$, $K_8U_3Mo_5O_{28}$, $K_{10}U_4$ Mo_4O_{29}, $K_6U_7Mo_5O_{33}$ and $K_4U_3Mo_2O_{17}$. In the Cs–U–Mo–O system, preparation, thermal behaviour and luminescence spectra of $Cs_2UO_2(MoO_4)_2$, $Cs_2(UO_2)_2(MoO_4)_3$ and $Cs_6(UO_2)(MoO_4)_4$ compounds have been reported by Krasovskaya et al. [4] and X-ray and thermal studies of $Cs_2UO_2(MoO_4)_2$ and $Cs_2(UO_2)_2(MoO_4)_3$ by Misra et al. [5]. The Rb–U–Mo–O system have been studied by Tatarinova and Sadikove et al. [6,7]. The preparation, X-ray, thermal and IR studies of $Rb_2UO_2(MoO_4)_2$ and $Rb_2(UO_2)_2(MoO_4)_3$ have been reported by Chawla et al. [8].

Even though considerable work has been reported on the ternaries, Na–Mo–O [9], Na–U–O [10] and U–Mo–O [11,12], very limited structural and thermal information is available on the Na–U–Mo–O quaternary system. For the Na–U–Mo–O system, Dion and Noel [13] prepared Na_2-$U_3Mo_4O_{22}$, $Na_2UMo_2O_{10}$, $Na_4U_3Mo_2O_{17}$, Na_2-$U_3Mo_9O_{37}$ and $Na_2UMo_4O_{16}$ and identified these phases by X-ray diffraction, but the data were not indexed. Further, in the literature, no thermal data is available on compounds of the Na–U–Mo–O quaternary system. In this paper we describe the preparation and characterization of the quaternary compounds, $Na_2UMo_2O_{10}$, $Na_2U_2Mo_2O_{13}$, Na_2-$U_2Mo_3O_{16}$, $Na_2UMo_4O_{16}$ and $Na_2U_2Mo_4O_{19}$ and also obtain a pseudo-ternary phase diagram of Na_2O–UO_3–MoO_3 system.

2. Experimental

2.1. Sample preparation

Na_2MoO_4 and MoO_3 (both available in A.R. grade) were used as starting materials for the preparation of higher sodium molybdates. The compounds $Na_2Mo_2O_7$ and $Na_2Mo_4O_{13}$ were prepared by heating mixtures of Na_2MoO_4 and MoO_3 in a platinum boat, in air, in molar ratios 1:1 at 650 °C [14] and 1:3 at 550 °C [15], respectively, followed by quenching. UO_3 was prepared from ammonium diuranate (ADU) precipitates by adding ammonia to uranyl nitrate (nuclear pure) solution and then decomposing at 350 °C. Similarly, uranyl molybdate, UO_2MoO_4, was prepared by heating a reaction mixture of UO_2 (Nuclear Grade from Uranium Metal Plant, BARC) and MoO_3 in a molar ratio of 1:1 in a platinum boat at 800 °C for 40 h [16].

In Na–U–Mo–O quaternary system, $Na_2UMo_2O_{10}$ and $Na_2U_2Mo_2O_{13}$ were prepared by heating mixtures of $Na_2Mo_2O_7$ and UO_3 in alumina boats, in 1:1 and 1:2 molar ratios respectively, in air at 550 °C for 12–14 h with intermittent grinding. $Na_2U_2Mo_3O_{16}$ was prepared by heating a mixture of $Na_2Mo_2O_7$, UO_3 and MoO_3 at a ratio, of 1:2:1 in air for 12–15 h at 550 °C. The compounds $Na_2UMo_2O_{10}$ and $Na_2U_2Mo_3O_{16}$ were obtained by heating an appropriate mixture of Na_2MoO_4 and UO_2MoO_4 at 550 °C in air. $Na_2UMo_4O_{16}$ and $Na_2U_2Mo_4O_{19}$, were prepared by heating mixtures of $Na_2Mo_4O_{13}$ and UO_3, in mole ratios of 1:1 and 1:2, respectively, at 500 °C and 550 °C in air. To get the homogeneous products, all the reaction mixtures were thoroughly mixed and grounded in pestle and mortar before heating at the desired temperatures.

The formation of these compounds can be summarized as

$$Na_2Mo_2O_7 + UO_3 \rightarrow Na_2UMo_2O_{10} \quad (1)$$

$$Na_2MoO_4 + UO_2MoO_4 \rightarrow Na_2UMo_2O_{10} \quad (2)$$

$$Na_2Mo_2O_7 + 2UO_3 \rightarrow Na_2U_2Mo_2O_{13} \quad (3)$$

$$Na_2Mo_2O_7 + 2UO_3 + MoO_3 \rightarrow Na_2U_2Mo_3O_{16} \quad (4)$$

$$Na_2MoO_4 + 2UO_2MoO_4 \rightarrow Na_2U_2Mo_3O_{16} \quad (5)$$

$$Na_2Mo_4O_{13} + UO_3 \rightarrow Na_2UMo_4O_{16} \quad (6)$$

$$Na_2Mo_4O_{13} + 2UO_3 \rightarrow Na_2U_2Mo_4O_{19} \quad (7)$$

Similarly, solid state reactions of UO_3 with $Na_2Mo_2O_7$ and $Na_2Mo_4O_{13}$ were performed in stoichiometric proportions at 550 °C in air, yielding $Na_2U_3Mo_2O_{16}$ and $Na_2U_3Mo_4O_{22}$, respectively, as reported by Dion and Noel [13].

The mole fraction ratios of Na_2MoO_4, UO_3 and MoO_3, used for the preparation of the above five quaternary compounds and the 17 phase mixtures, prepared for obtaining the phase diagram, are given in Table 1. Seventeen phase mixtures were heated at 550 °C in air for 12–14 h.

2.2. Instrumental analysis

The progress of all the reactions and the formation of the various products were monitored by recording X-ray diffraction (XRD) patterns at 6°/min, on a DIANO X-ray diffractometer using Cu $K_{\alpha}1$ ($\lambda = 0.154056$ nm). To obtain cell parameters, XRD data were recorded at 1°/min.

Infrared spectra were recorded for all the sodium uranyl molybdates in the range of 400–4000 cm^{-1}

Table 1
Phase identification of various compounds in Na_2O–UO_3–MoO_3

Mixture number	Mole fraction of the oxides			Phase identified		
	Na_2O	UO_3	MoO_3			
A	0.25	0.25	0.50		$Na_2UMo_2O_{10}$	
B	0.20	0.40	0.40		$Na_2U_2Mo_2O_{13}$	
C	0.17	0.33	0.50		$Na_2U_2Mo_3O_{16}$	
D	0.17	0.17	0.66		$Na_2UMo_4O_{16}$	
E	0.14	0.29	0.57		$Na_2U_2Mo_4O_{19}$	
N1	0.07	0.23	0.70	E	UO_2MoO_4	MoO_3
N2	0.22	0.07	0.71	D	$Na_2Mo_2O_7$	$Na_2Mo_4O_{13}$
N3	0.10	0.33	0.57	E	UO_2MoO_4	MoO_3
N4	0.25	0.13	0.62	A	D	$Na_2Mo_2O_7$
N5	0.10	0.60	0.30	B	UO_2MoO_4	UO_3
N6	0.11	0.35	0.54	E	C	UO_2MoO_4
N7	0.17	0.50	0.33	B	UO_3	–
N8	0.13	0.37	0.50	C	UO_2MoO_4	–
N9	0.14	0.20	0.66	E	D	MoO_3
N10	0.13	0.07	0.80	D	MoO_3	$Na_2Mo_4O_{13}$
N11	0.35	0.10	0.55	A	Na_2MoO_4	$Na_2Mo_2O_7$
N12	0.27	0.27	0.46	A	B	Na_2MoO_4
N13	0.20	0.25	0.55	A	C	D
N14	0.20	0.33	0.47	A	B	C
N15	0.17	0.60	0.23	B	Na_2MoO_4	UO_3
N16	0.30	0.30	0.40	B	Na_2MoO_4	UO_3
N17	0.16	0.26	0.58	E	C	D

on a JASCO (Japan) FT/IR-610 spectrometer, in Nujol mulls and on KBr disc.

Thermograms of the above five pure compounds prepared here were recorded on a ULVAC Thermoanalyzer, recording thermogravimetric (TG) and differential thermal analysis (DTA) curves simultaneously. Samples were heated and cooled in platinum cups at 10 °C/min in flowing dry air. Preheated alumina was the reference material for DTA measurements.

3. Results and discussion

3.1. X-ray diffraction studies

X-ray diffraction patterns of $Na_2UMo_2O_{10}$, $Na_2U_2Mo_2O_{13}$, $Na_2U_2Mo_3O_{16}$, $Na_2UMo_4O_{16}$ and $Na_2U_2Mo_4O_{19}$ showed the absence of lines corresponding to the starting compounds, thus confirming the formation of pure compounds. In all the tables and figures these compounds are labeled as 'A', 'B', 'C', 'D' and 'E', respectively. Dion and Noel [13] reported the preparation and XRD studies of α-$Na_2UMo_2O_{10}$ and β-$Na_2UMo_2O_{10}$ phases, but the data are assigned '0' values as the data was not indexed. The XRD data of all the molybdate compounds were indexed on the orthorhombic system and the cell parameters were refined by a least squares method using a computer program [17]. The refined cell parameters of all five compounds are given in Table 2. The densities of $Na_2UMo_2O_{10}$, $Na_2U_2Mo_2O_{13}$, $Na_2U_2Mo_3O_{16}$, $Na_2UMo_4O_{16}$ and $Na_2U_2Mo_4O_{19}$ were determined, by a pycnometric

Table 2
Crystal data of new compounds prepared and indexed on orthorhombic system

Compound	Cell parameters (nm)	Density (g/cm^3)		*Z*
		Calculated	Measured	
$Na_2UMo_2O_{10}$	$a = 0.6923(5)$ $b = 1.7785(10)$ $c = 1.2998(7)$	2.76	2.70	4
$Na_2U_2Mo_2O_{13}$	$a = 0.7761(4)$ $b = 1.6747(1)$ $c = 1.2159(7)$	3.12	2.90	4
$Na_2U_2Mo_3O_{16}$	$a = 1.7368(2)$ $b = 0.8952(1)$ $c = 1.2750(9)$	3.60	3.57	4
$Na_2UMo_4O_{16}$	$a = 0.6119(4)$ $b = 1.3528(4)$ $c = 2.0075(4)$	2.00	1.88	2
$Na_2U_2Mo_4O_{19}$	$a = 0.8833(2)$ $b = 1.4128(5)$ $c = 0.9709(2)$	3.32	3.34	2

method using carbon tetrachloride as a solvent. The measured and calculated densities of the compounds are also included in Table 2. The indexed XRD data of $Na_2UMo_2O_{10}$, $Na_2U_2Mo_2O_{13}$, $Na_2U_2Mo_3O_{16}$, $Na_2UMo_4O_{16}$ and $Na_2U_2Mo_4O_{19}$ are given in Tables 3–7, respectively.

Dion and Noel [13] have reported the existence of $Na_2U_3Mo_2O_{16}$ and $Na_2U_3Mo_4O_{22}$, but we observed that the compounds $Na_2U_3Mo_2O_{16}$ and $Na_2U_3Mo_4O_{22}$ were in-fact mixtures of $Na_2U_2Mo_2O_{13} + UO_2MoO_4$ and $Na_2U_2Mo_4O_{19} + UO_2MoO_4$, respectively, from XRD data.

Table 3
XRD data of $Na_2UMo_2O_{10}$ ($\lambda = 0.154056$ nm)

h	k	l	d(obs)	d(cal)	I/I_0
0	2	0	0.8870	0.8890	100
1	1	0	0.6453	0.6450	15
0	1	2	0.6104	0.6100	70
1	1	1	0.5785	0.5770	5
1	2	0	0.5498	0.5460	5
1	2	1	0.5035	0.5030	<5
1	0	2	0.4767	0.4730	5
0	4	0	0.4437	0.4440	30
0	0	3	0.4308	0.4330	5
0	2	3	0.3891	0.3890	5
1	4	0	0.3731	0.3740	20
0	3	3	0.3497	0.3490	5
1	2	3	0.3386	0.3390	15
2	1	1	0.3281	0.3280	35
2	2	1	0.3129	0.3130	5
2	0	2	0.3054	0.3050	30
0	6	0	0.2962	0.2960	<5
0	3	4	0.2851	0.2850	15
0	5	3	0.2757	0.2740	5
0	7	0	0.2536	0.2540	<5
1	1	5	0.2406	0.2410	<5
3	0	3	0.2038	0.2030	5
0	9	0	0.1976	0.1970	<5
0	0	7	0.1857	0.1850	<5
3	3	4	0.1793	0.1790	<5
3	1	5	0.1718	0.1710	<5
0	8	5	0.1690	0.1690	<5
2	9	3	0.1597	0.1590	<5
1	3	8	0.1529	0.1520	<5

Table 4
XRD data of $Na_2U_2Mo_2O_{13}$ ($\lambda = 0.154056$ nm)

h	k	l	d(obs)	d(cal)	I/I_0
0	2	0	0.8419	0.8377	11
1	1	0	0.7066	0.7048	7
1	1	1	0.6102	0.6100	100
0	3	0	0.5566	0.5584	7
1	2	1	0.5162	0.5159	7
0	2	2	0.4939	0.4925	14
1	3	2	0.3640	0.3637	6
1	4	1	0.3528	0.3528	7
1	2	3	0.3301	0.3305	6
0	5	1	0.3230	0.3231	26
2	2	2	0.3048	0.3050	46
3	3	3	0.2033	0.2033	11

Table 5
XRD data of $Na_2U_2Mo_3O_{16}$ ($\lambda = 0.154056$ nm)

h	k	l	d(obs)	d(cal)	I/I_0
0	1	0	0.8950	0.8952	100
2	0	1	0.7144	0.7177	10
1	0	2	0.5971	0.5985	17
2	1	1	0.5616	0.5600	17
0	1	2	0.5189	0.5193	12
1	1	2	0.4975	0.4975	19
2	1	2	0.4458	0.4457	15
0	2	1	0.4200	0.4223	11
2	2	0	0.3972	0.3979	14
1	1	3	0.3747	0.3749	15
0	2	2	0.3666	0.3663	22
3	2	0	0.3548	0.3541	14
4	1	2	0.3322	0.3331	25
5	1	0	0.3241	0.3238	20
4	1	3	0.2875	0.2876	15
4	0	4	0.2570	0.2569	11
4	3	2	0.2297	0.2295	8
0	2	6	0.1920	0.1920	8
3	2	6	0.1823	0.1822	10

Table 6
XRD data of $Na_2UMo_4O_{16}$ ($\lambda = 0.154056$ nm)

h	k	l	d(obs)	d(cal)	I/I_0
0	2	0	0.6763	0.6764	36
1	1	0	0.5568	0.5576	10
1	0	2	0.5224	0.5225	12
1	2	2	0.4134	0.4135	100
0	3	4	0.3353	0.3354	56
1	3	3	0.3188	0.3191	80
1	2	5	0.3009	0.3007	9
1	0	7	0.2599	0.2597	13
2	3	1	0.2511	0.2512	11
0	0	9	0.2231	0.2231	10
1	1	7	0.2061	0.2060	19
0	7	1	0.1923	0.1924	7
0	3	10	0.1834	0.1834	10
0	0	12	0.1672	0.1673	8
2	7	3	0.1588	0.1587	7

3.2. Infrared spectra of sodium uranyl molybdates

The IR spectra of all the sodium uranyl molybdates are shown in Fig. 1 and the corresponding vibrations are given in Table 8. The spectral bands in the region of 700–950 cm^{-1} were due to the presence of MoO_4^{2-} tetrahedra groups. The IR spectra of

Table 7
XRD data of $Na_2U_2Mo_4O_{19}$ ($\lambda = 0.154056$ nm)

h	k	l	d(obs)	d(cal)	I/I_0
0	2	0	0.7053	0.7065	33
2	1	0	0.4217	0.4216	26
1	1	2	0.4075	0.4074	68
1	3	2	0.3158	0.3157	100
3	3	0	0.2495	0.2497	40
2	1	4	0.2102	0.2104	15
2	2	4	0.2037	0.2037	16
4	2	2	0.1934	0.1934	15
0	5	4	0.1842	0.1841	24
1	7	2	0.1824	0.1824	20
5	2	0	0.1714	0.1714	19
2	3	5	0.1663	0.1663	17
2	6	4	0.1578	0.1579	15

alkali metal molybdates, potassium uranyl molybdate and sodium uranyl molybdates also show the spectral bands in the same regions due to the MoO_4^{2-} tetrahedra [18–20]. The spectral bands from 905–920 cm^{-1} were observed due to the presence of UO_2^{2+} group [19].

3.3. TG and DTA studies of sodium uranyl molybdates

TG curves of $Na_2UMo_2O_{10}$, $Na_2U_2Mo_2O_{13}$, $Na_2U_2Mo_3O_{16}$, $Na_2UMo_4O_{16}$ and $Na_2U_2Mo_4O_{19}$ did not show any weight change up to 600 °C, indicating that these compounds do not undergo any compositional changes up to 600 °C.

Heating and cooling DTA curves of $Na_2UMo_2O_{10}$ are shown in Fig. 2(A). On heating, the DTA curve of $Na_2UMo_2O_{10}$ showed two endothermic peaks. The first, at 550 °C is attributed to a reversible phase change and the second at 590 °C to the melting of $Na_2UMo_2O_{10}$. On controlled

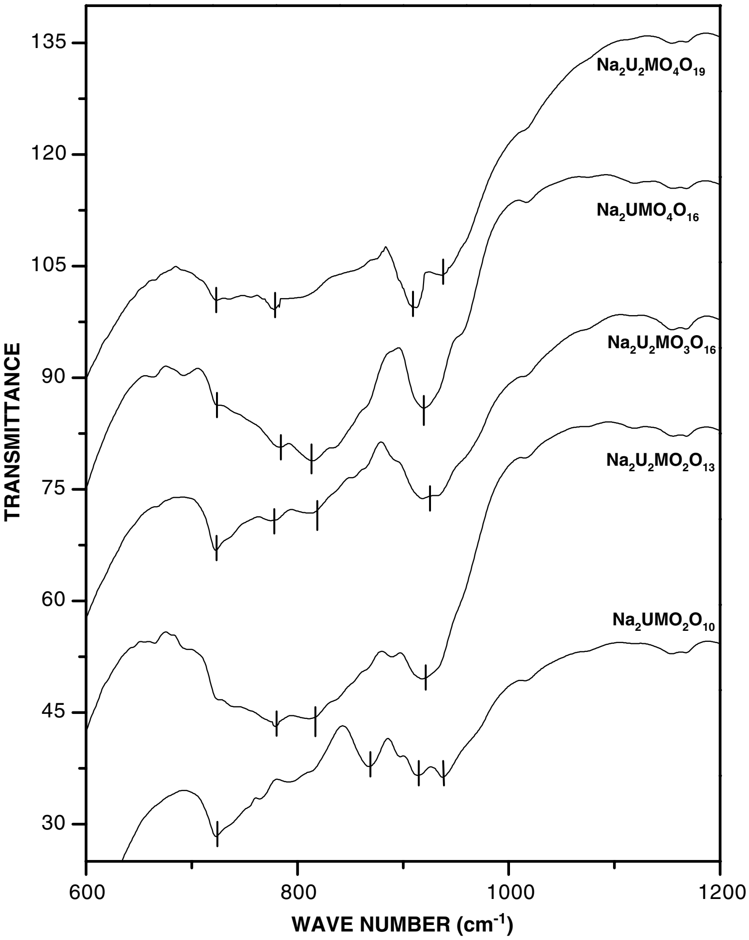

Fig. 1. FTIR spectra of sodium uranyl molybdates.

Table 8
FTIR spectra of sodium uranyl molybdates

Compounds	MoO_4^{2-} (cm^{-1})	UO_2^{2+} (cm^{-1})
$Na_2UMo_2O_{10}$	723, 764, 867, 937	914
$Na_2U_2Mo_2O_{13}$	779, 811	919
$Na_2U_2Mo_3O_{16}$	723, 775, 812	918
$Na_2UMo_4O_{16}$	722, 760, 810	916
$Na_2U_2Mo_4O_{19}$	723, 777, 933	909

cooling, in air, at 10 °C/min, two sharp exothermic DTA peaks were observed at 535 °C and 470 °C, due to crystallization and the a reversible phase change, respectively. The XRD patterns of $Na_2UMo_2O_{10}$, both before and after this heating–cooling cycle were identical.

In Fig. 2(B), the heating DTA curve of $Na_2U_2Mo_2O_{13}$ showed an endothermic peak at 580 °C due to melting. The cooling curve showed an exothermic peak at 480 °C, due to crystallization. The XRD patterns before and after the heating and cooling cycle were the same.

The DTA curve of $Na_2U_2Mo_3O_{16}$ given in Fig. 2(C), showed two endothermic peaks upon heating, at 515 °C and 570 °C, due to a phase change and melting, respectively and the cooling curve shows only one exothermic DTA peak at 545 °C. The peak area obtained during DTA cooling, was approximately equal to the area under the two heating DTA peaks. Therefore, single peak during cooling may be due to the overlapping of two transition peaks. The XRD patterns before and after melting were also different in this case. The XRD pattern of the sample obtained after the DTA experiments showed lines for $Na_2U_2Mo_3O_{16}$ and some lines corresponding to the higher melting quaternary compound, $Na_2UMo_2O_{10}$ and a stable

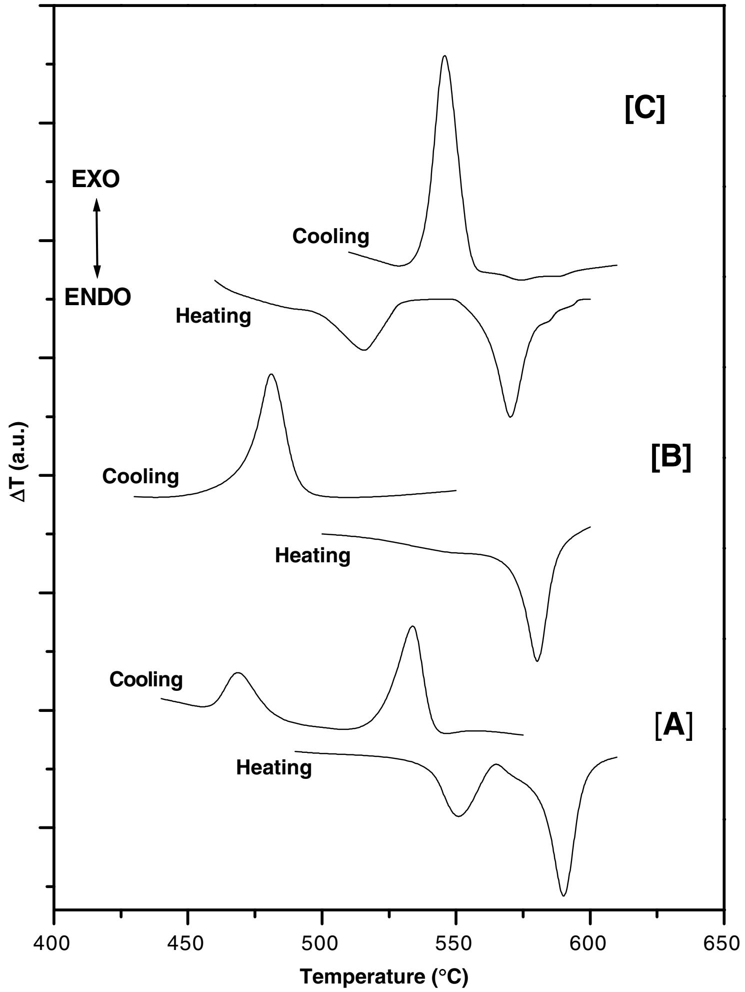

Fig. 2. Heating and cooling DTA curves of (A) $Na_2UMo_2O_{10}$, (B) $Na_2U_2Mo_2O_{13}$ and (C) $Na_2U_2Mo_3O_{16}$ recorded in air.

ternary compound, UO_2MoO_4. The appearance of these two new phases may be due to high stability of the ternary compound, UO_2MoO_4, which has a high melting point. Therefore, the melt of $Na_2U_2Mo_3O_{16}$ may have some short range ordering corresponding to UO_2MoO_4. During fast DTA cooling, due to sluggish kinetics of quaternary phase transitions, some UO_2MoO_4 compound might have precipitated along with $Na_2U_2Mo_3O_{16}$. To maintain the mass balance of the system, another stable compound $Na_2UMo_2O_{10}$, was also formed. This can explain the presence of XRD lines for these three compounds of the UO_2MoO_4–Na_2MoO_4 pseudo-binary system.

DTA curves obtained during heating and cooling of $Na_2UMo_4O_{16}$ are shown in Fig. 3(D). While heating in air, the DTA curve of $Na_2UMo_4O_{16}$ showed two endothermic peaks, at 470 °C due to the solid–solid reversible phase change and at 510 °C, due to melting. On cooling DTA curve showed these two peaks at 470 °C and 410 °C, shifted to lower temperatures, as expected. In the case of $Na_2UMo_4O_{16}$, XRD patterns before and after DTA experiments were found to be identical.

DTA curves of $Na_2U_2Mo_4O_{19}$ obtained during the heating and cooling cycles are given in Fig. 3(E). The heating curve showed two endothermic peaks, at 515 °C and 560 °C, due to a solid–solid phase change and melting, respectively. During cooling these two transitions shifted to 515 °C and 440 °C. The XRD pattern of $Na_2U_2Mo_4O_{19}$, after DTA experiment contained the additional XRD lines of UO_2MoO_4. This also may be due to the phenomenon similar to that observed in $Na_2U_2Mo_3O_{16}$, as discussed earlier. Due to slow kinetics and fast cooling rates, the equilibria were

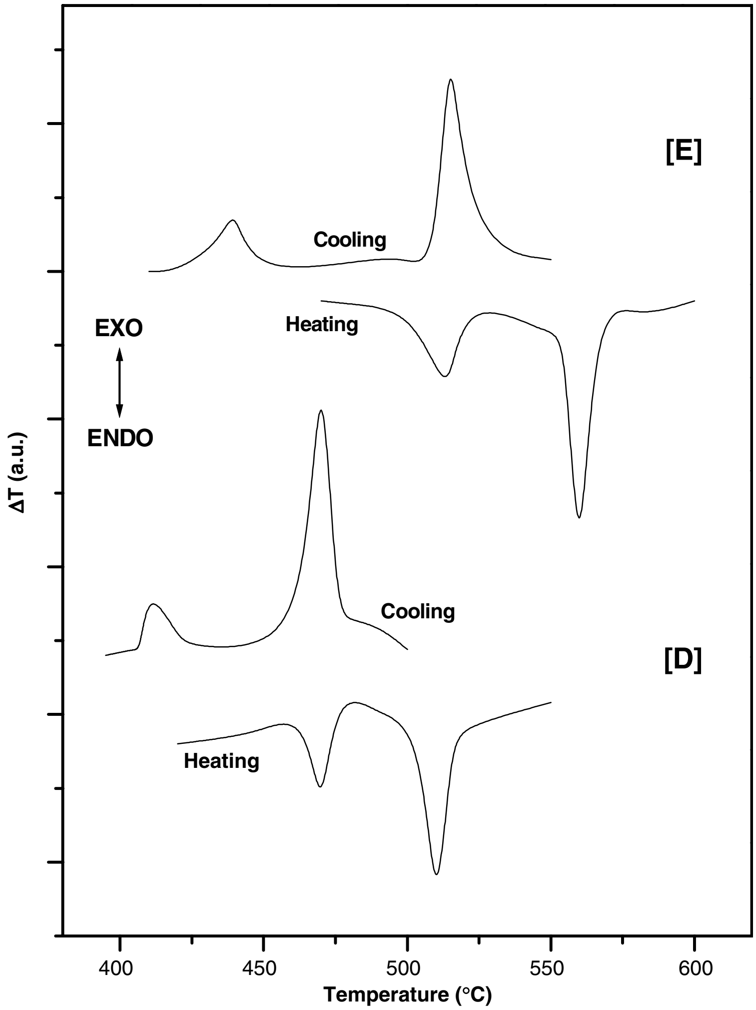

Fig. 3. Heating and cooling DTA curves of (D) $Na_2UMo_4O_{16}$ and (E) $Na_2U_2Mo_4O_{19}$ recorded in air.

not attained during DTA cooling runs and more stable neighbouring compounds tended to precipitate out. However, according to mass balance considerations, another compound richer in Na_2O than Na_2-$U_2Mo_4O_{19}$, should have also appeared, corresponding to the pseudo-binary, $Na_2Mo_2O_7$. It is possible that $Na_2Mo_2O_7$ was also present in the samples obtained after DTA experiments but the corresponding XRD lines were not observed as this low melting compound easily freezes into glassy phase.

When the samples of sodium uranyl molybdates were heated at 950 °C for 14–16 h, they all decomposed to sodium diuranate $Na_2U_2O_7$, confirmed by comparing the X-ray data with that reported in the literature [21]. Another decomposition product is MoO_3, however, MoO_3 starts vaporizing above 770 °C [22], therefore no detectable traces of MoO_3 were left in the samples after heating them at 950 °C. Bright needle like crystals of MoO_3 were observed in the cooler region of the reaction tube of the furnace, which was confirmed by XRD.

The phase transition temperatures in the heating and cooling DTA curves of $Na_2UMo_2O_{10}$, Na_2-$U_2Mo_2O_{13}$, $Na_2U_2Mo_3O_{16}$, $Na_2UMo_4O_{16}$ and $Na_2U_2Mo_4O_{19}$ were different, a common phenomenon, even in perfectly reversible transitions. It depends upon the kinetics of the phase transitions. Kinetically slow transitions result in super cooling or superheating during DTA runs. The lack of an internal equilibrium and unequal temperature distribution within the sample can also contribute to this phenomenon of different transition temperatures on heating and cooling as reported in case of Na_2-$Pu(MoO_4)_3$, $Tl_2Pu(MoO_4)_3$, $Tl_4Pu(MoO_4)_4$, $Tl_2Th(MoO_4)_3$ and $Tl_4Th(MoO_4)_4$ [23,24].

4. Phase diagram studies

The three systems, Na_2O–UO_3, UO_3–MoO_3 and Na_2O–MoO_3 were used for establishing the pseudo-ternary phase diagram of the Na_2O–UO_3–MoO_3 system, as shown in Fig. 4. The system Na_2O–MoO_3 has three ternary compounds, Na_2MoO_4, $Na_2Mo_4O_{13}$ and $Na_2Mo_2O_7$ [14,15,25]. Recently the high temperature studies of Na_2MoO_4, $Na_2Mo_4O_{13}$ and $Na_2Mo_2O_7$ were carried out in our laboratory using STOE X-ray diffractometer and the XRD data reported by us [26] is in good agreement with the literature data. In UO_3–MoO_3 system only one compound UO_2MoO_4 is reported in the literature [16]. The '*d*' values of UO_2MoO_4 obtained by us are in good agreement with the literature values, as shown in Table 9. The important *d*-values of Na_2MoO_4, $Na_2Mo_2O_7$, $Na_2Mo_4O_{13}$, UO_2MoO_4, UO_3 and MoO_3 [27,28] are given in Table 10.

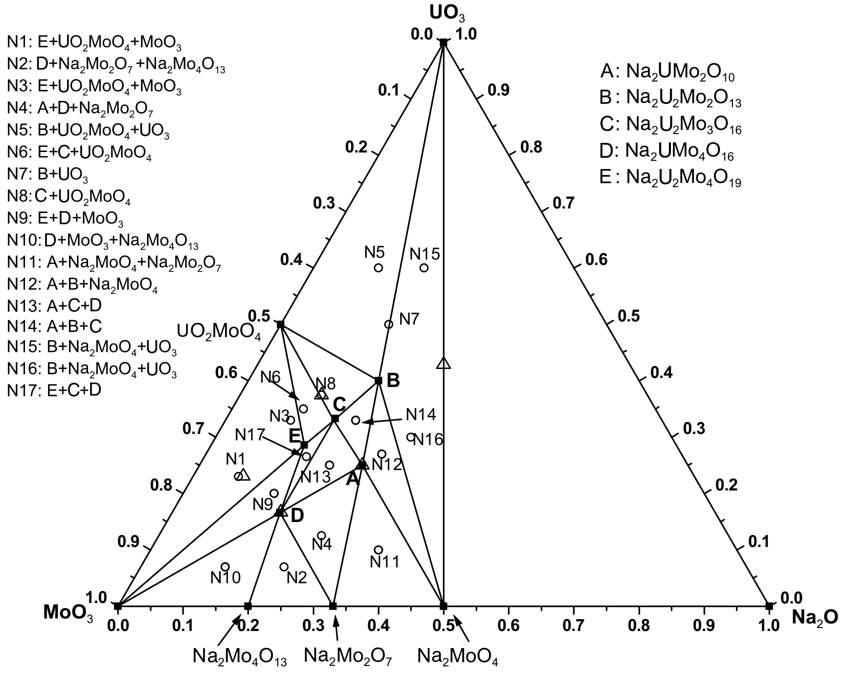

Fig. 4. Isothermal section of pseudo-ternary phase diagram of Na_2O–UO_3–MoO_3 system at 550 °C.

Table 9
Comparison of observed and reported XRD patterns for UO_2MoO_4

Observed *d* values (nm)	Relative intensity	Reported *d* values (nm)[a]	Relative intensity
0.6978	18	0.6936	25
0.5527	10	0.5523	26
0.4305	38	0.4308	29
0.4213	100	0.4210	100
0.3917	35	0.3918	49
0.3482	20	0.3482	21
0.3349	18	0.3343	23
0.3288	37	0.3286	28
0.2939	18	0.2939	17
0.2834	<5	0.2834	<5
0.2738	<5	0.2742	<5
0.2549	20	0.2549	14
0.2456	10	0.2456	8
0.2308	5	0.2308	5
0.2189	<5	0.2187	7
0.2122	18	0.2121	14
0.2036	10	0.2034	9
0.1994	<5	0.1991	5
0.1922	<5	0.1921	5
0.1843	<5	0.1840	7
0.1810	5	0.1810	<5
0.1768	5	0.1768	<5
0.1738	7	0.1738	5
0.1688	7	0.1687	<5

[a] PDF card no. [72-778].

Though there are many ternary compounds reported for the $Na_2O–UO_3$ system, none were relevant to the partial quaternary phase diagram studied in the present work.

Dion and Noel [13] reported five compounds in the partial phase diagram studied here (x_{Na_2O}: $x_{MoO_3} \leqslant 1:1$), viz., $Na_2U_3Mo_4O_{22}$, $Na_2UMo_2O_{10}$, $Na_4U_3Mo_2O_{17}$, $Na_2U_3Mo_9O_{37}$ and $Na_2UMo_4O_{16}$ containing Na_2O, UO_3 and MoO_3 in the ratios, $(Na_2O)(UO_3)_3(MoO_3)_4$, $(Na_2O)(UO_3)(MoO_3)_2$, $(Na_2O)_2(UO_3)_3(MoO_3)_2$, $(Na_2O)(UO_3)_3(MoO_3)_9$, $(Na_2O)(UO_3)(MoO_3)_4$. Of these, $Na_2UMo_4O_{16}$ and $Na_2UMo_2O_{10}$, were found to be pure compounds during the present studies. However, other compounds, $Na_4U_3Mo_2O_{17}$, $Na_2U_3Mo_9O_{37}$ and $Na_2U_3Mo_4O_{22}$ were found to be mixtures of $UO_3 + Na_2MoO_4 + Na_2U_2Mo_2O_{13}$, $UO_2MoO_4 + UO_3 + Na_2U_2Mo_4O_{19}$ and $UO_2MoO_4 + Na_2U_2Mo_3O_{16} + Na_2U_2Mo_2O_{13}$, respectively. The quaternary compounds found in these mixtures, $Na_2U_2Mo_2O_{13}$, $Na_2U_2Mo_4O_{19}$ and $Na_2U_2Mo_3O_{16}$ were identified and indexed for the first time in the present work, as discussed in previous section. Due to this discrepancy between the present work and that reported by Dion and Noel [13], on the stable quaternary compounds, it became necessary to re-establish the phase-diagram of $Na_2O–UO_3–MoO_3$ system. Therefore, all the tentative phase diagrams with possible phase fields were drawn. Using these diagrams, 17 samples of relevant compositions with different mole fractions of Na_2O, UO_3 and MoO_3 were prepared. The phases determined by XRD analysis of these compositions were used for drawing the final phase boundaries. These compositions along with detected phases are listed in Table 1. The partial phase diagram of the system $Na_2O–UO_3–MoO_3$, drawn using this information is given in Fig. 4. The compositions examined by XRD for phase-field determination are given as open circles in the figure, the pure compounds, quaternary as well as ternary compounds are given as filled squares and the pseudo ternary compounds given by Dion and Noel [13] are given as open triangles.

Acknowledgements

The authors are thankful to Dr V. Venugopal, Director, Radiochemistry and Isotope Group and Dr S.K. Aggarwal, Head, FCD for their keen interest in this work. The authors are also thankful to Dr K.V. Chetty for recording the IR spectra of all the sodium uranyl molybdate compounds.

Table 10
X-ray powder diffraction data of the compounds in $Na_2O–MoO_3$ and $UO_3–MoO_3$ systems, used in the present work

Compounds	*d* values (nm)[a]										Ref.
UO_3	0.345_{10}	0.326_6	0.498_5	0.439_4	0.437_3	0.306_2	0.280_3	0.279_3	0.174_3	0.306_2	[27]
MoO_3	0.326_{10}	0.381_8	0.346_6	0.266_4	0.693_3	0.231_3	0.270_2	0.227_2	0.196_2	0.185_2	[28]
UO_2MoO_4	0.421_{10}	0.392_3	0.431	0.329_2	0.552_2	0.694_2	0.334_2	0.348_2	0.294_2	0.255_1	[16]
Na_2MoO_4	0.274_{10}	0.322_9	0.526_7	0.161_4	0.186_4	0.175_4	0.119_2	0.144_1	0.122_1	0.154_1	[24]
$Na_2Mo_2O_7$	0.549_{10}	0.306_9	0.471_9	0.313_8	0.322_7	0.315_7	0.378_5	0.461_4	0.300_4	0.736_3	[14]
$Na_2Mo_4O_{13}$	0.555_{10}	0.346_6	0.231_6	0.313_5	0.690_5	0.328_5	0.764_4	0.380_4	0.336_4	0.298_4	[15]

[a] Ten strong lines in descending order of intensity (given as subscripts).

References

[1] R.S. Fidler, M.J. Collins, At. Energy Rev. 13 (1975) 3.

[2] C. Dion, A. Noel, Bull. Soc. Chim. Fr. (1983) 257.

[3] C. Dion, A. Noel, Bull. Soc. Chim. Fr. (1985) 735.

[4] T.I. Krasovskaya, Yu.A. Polyakov, I.A. Rozanova, Izv. Akad. Nauk. SSSR 16 (1980) 1824.

[5] N.L. Misra, K.L. Chawala, N.C. Jayadevan, D.D. Sood, J. Nucl. Mater. 226 (1995) 120.

[6] E. Tatarinova, Sov. Radiochem. (English Translation) 33 (1991) 258.

[7] G.G. Sadikove, T.I. Krasovskaya, Yu.A. Polyakov, V.P. Nikolaev, Izv. Akad. Nauk., SSSR, Neorg. Mater. 24 (1988) 109.

[8] K.L. Chawala, N.L. Misra, N.D. Dahale, N.C. Jayadevan, in: Proc. Ninth National Symp. on Thermal Analysis, Goa, 1993, p. 321.

[9] T. Gyanshekharan, K.H. Mahendran, K.V.G. Kutty, C.K. Mathews, J. Nucl. Mater. 165 (1989) 210.

[10] H.K. Kleykamp, Report KFK-4701, 1990;
H. Kleykamp, Nucl. Technol. 80 (1988) 412.

[11] V.K. Trunov, O.N. Rozanova, L.M. Kovba, J. Inorg. Chem. 10 (1965) 1400.

[12] G. Chattopadhyay, S.N. Tripathi, A.S. Kerkar, J. Am. Ceram. Soc. 67 (1984) 610.

[13] C. Dion, A. Noel, Bull. Soc. Chim. Fr. (1977) 1115;
C. Dion, A. Noel, Bull. Soc. Chim. Fr. (1981) 185;
C. Dion, A. Noel, Bull. Soc. Chim. Fr. (1982) 188.

[14] M. Seleborg, Acta Chem. Scand. 21 (1967) 499.

[15] M. Balashov, Inorg. Mater. (English Translation) 6 (1970) 1276, JCPDF card no. 28-1112.

[16] V.N. Serezhkin, L.M. Kovba, V.K. Trunov, Kristallografiya 17 (1972) 1127.

[17] LATPAR, A least squares program written by V.K. Wadhavan, Neutron Physics Division, Bhabha Atomic Research Centre, Mumbai, India.

[18] C. Dion, Bull. Soc. Chim. Fr. (1) (1989) 42.

[19] A.M. Fedoseev, N.A. Budantseva, A.B. Yusov, M.S. Grigor, T.I. Potemkina, Radiokhimija. 32 (1990) 14.

[20] G.M. Clark, W.P. Doyle, Spectrochim. Acta 22 (1966) 1441.

[21] PDF No. 43-347, International Centre for Diffraction Data, Newtown Square, USA.

[22] M.S. Saamant, P.N. Namoodiri, S.R. Dharwadkar, Mater. Chem. Phys. 35 (1993) 120.

[23] Smruti Dash, Ziley Singh, N.D. Dahale, R. Prasad, V. Venugopal, J. Alloys Compd. 347 (2002) 301.

[24] N.D. Dahale, Meera Keskar, K.D. Singh Mudher, J. Alloys Compd. 415 (2006) 244.

[25] PDF No. 5-0508, International Centre for Diffraction Data, Newtown Square, USA.

[26] K.D. Singh Mudher, Meera Keskar, K. Krishnan, V. Venugopal, J. Alloys Compd. 396 (2005) 275.

[27] PDF No.31-1423, International Centre for Diffraction Data, Newtown Square, USA.

[28] PDF No. 5-0508, International Centre for Diffraction Data, Newtown Square, USA.